

The Comparative Study in the Oxygen Atom Transfer Reaction by Ruthenium Mono-Oxo Complexes

Won K. Seok, Yung J. Son, Sung W. Moon, and Heung N. Lee

Department of Chemistry, Dongguk University, 26 Pil-Dong, Chung-Ku, Seoul 100-715, Korea

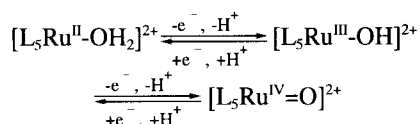
Received June 18, 1998

The oxidation of triphenylphosphine by $[(\text{tpy})(\text{phen})\text{Ru}^{\text{IV}}(\text{O})]^{2+}$ and $[(\text{bpy})(p\text{-tert-butylpy})\text{Ru}^{\text{IV}}(\text{O})]^{2+}$ (tpy is 2,2':6',2''-terpyridine, phen is 1,10-phenanthroline, bpy is 2,2'-bipyridine, and *p-tert-butylpy* is *para-tert-butylpyridine*) in CH_3CN has been studied. Experiments using ^{18}O -labeled complex show the oxyl group transfer from $[\text{Ru}^{\text{IV}}=\text{O}]^{2+}$ to triphenylphosphine occurred quantitatively within experimental error. Kinetic data were fit to a second-order for $[\text{Ru}^{\text{IV}}=\text{O}]^{2+}$ and $[\text{PPh}_3]$. The initial product, $[\text{Ru}^{\text{II}}\text{-OPPh}_3]^{2+}$, was formed as an observable intermediate and then underwent slow solvolysis. The reaction proceeded as endothermic in activation enthalpy and a decrease in activation entropy. The oxidative reactivity of four representative ruthenium mono-oxo oxidants against triphenylphosphine was compared. These systems have been utilized as electrochemical oxidative catalysts.

Introduction

Metal oxo complexes have been developed as new oxygen atom transfer reagents¹ and invoked as the reactive entities in metalloporphyrin-catalyzed epoxidations.² Dramatic progress in catalyzed epoxidation chemistry has been achieved in recent years with iodosylbenzene, peroxyacids, amine oxides, or hypochlorite anion as oxygen atom sources and porphyrin complexes of iron, chromium, and manganese as catalysts.³

A series of polypyridyl ruthenium aqua complexes have been known and a notable feature in their chemistry was the appearance of higher oxidation states obtained by the successive loss of proton and electron, which was accessible over a relatively narrow range in redox potentials.⁴



Crystal structures of complexes containing the $\text{Ru}(\text{IV})=\text{O}$ group showed that there was considerable ruthenium oxo multiple bond character arising from the electronic donation from the oxo group to $\text{Ru}(\text{IV})$.⁵

The oxo complexes of ruthenium with polypyridyl ligands have been shown to be efficient stoichiometric and/or catalytic oxidants toward inorganic and organic substrates.⁶ An important part of ruthenium mono-oxo complexes was the discovery of the extensive mechanistic and catalytic properties. In these d^4 complexes of the $\text{Ru}(\text{IV})$ -oxo group, the electron acceptor capability of the oxidant lay in the two vacancies in the d orbitals. It acted as a proton binding site or as a source of O^{2-} following electron transfer to the ruthenium metal.⁷

In the present work, we investigated the reactions between $\text{cis-}[\text{Ru}^{\text{IV}}(\text{bpy})(p\text{-tert-butylpy})(\text{O})]^{2+}$ and $\text{cis-}[\text{Ru}^{\text{IV}}(\text{tpy})(\text{phen})(\text{O})]^{2+}$ complexes and PPh_3 . We also wanted to establish the two-electron capability of the oxidants and to compare the reactivity of other known ruthenium mono-oxo oxidants.

Experimental Section

Materials. RuCl_3 , 2,2'-bipyridine(bpy), 2,2':6',2''-terpyridine(tpy), 1,10-phenanthroline (phen), AgClO_4 , $(\text{NH}_4)_2[\text{Ce}(\text{NO}_3)_6]$ (Ce(IV)), NH_4PF_6 , activated alumina, and SP-C-25 Sephadex were purchased from Aldrich Chemical Co. and used without further purification. Deuterium oxide (99.9% D, Aldrich Gold Label) and acetonitrile- d_3 (99.6% D, Aldrich Chemical Co.) were used as received. Triphenylphosphine was purchased from Aldrich Chemical Co., recrystallized twice from ethanol, and checked by FT-IR spectrophotometer to confirm the absence of "P=O" stretching frequency ($\nu_{\text{P=O}}=1195 \text{ cm}^{-1}$; nujol mull).⁸ Acetonitrile was purified by distillation from P_2O_5 under an Ar atmosphere. Distilled water was further purified by passing through a NanopureTM (Barnstead) water system. *Para-tert-butylpyridine*(*p-tert-butylpy*) was also obtained from Aldrich and purified according to a literature method.⁹ ^{18}O -labelled water (isotopic purity >97.1%) was purchased from Isotec, Inc. and used as received.

Preparations. $[\text{Ru}(\text{tpy})\text{Cl}_3]$, $[\text{Ru}(\text{bpy})_2(p\text{-tert-butylpy})(\text{OH}_2)](\text{ClO}_4)_2$, and $[\text{Ru}(\text{bpy})_2(p\text{-tert-butylpy})(\text{O})](\text{ClO}_4)_2$ were prepared by previously described procedures.^{6,7}

$[(\text{tpy})(\text{phen})\text{Ru}(\text{Cl})](\text{PF}_6)$. $\text{Ru}(\text{tpy})\text{Cl}_3$ (300 mg, 0.68 mmol, 1,10-phenanthroline (150 mg, 3.0 mmol), and LiCl (317 mg, 30.0 mmol) dissolved in 60 mL of ethanol and 20 mL of distilled water were heated at reflux under a stream of N_2 for 3h. After this period, the deep purple pot contents were filtered hot and reduced to *ca.* one-third of the original volume by evaporation. To the filtrate was added an excess of saturated NH_4PF_6 solution which resulted in the formation of a brown precipitate. The crude PF_6^- salt was dissolved in minimum CH_3CN followed by elution on a 1×20 cm column of alumina; eluent was 1:2 toluene-acetonitrile. The second purple band was evaporated to dryness to give a crystalline product. Yield: 319 mg (66%). Anal. Found (Calcd): C, 44.97 (45.49); H, 3.18 (2.97); N, 9.67 (9.82).

Caution! Care should be exercised in using a spatula or stirring rod to mechanically agitate any solid perchlorate.

These complexes, as well as other perchlorate salts, should be handled only in small quantities.

[(tpy)(phen)Ru(OH₂)](ClO₄)₂. [(tpy)(phen)Ru(Cl)](PF₆) (100 mg, 0.14 mmol) and AgClO₄ (31 mg, 0.15 mmol) were dissolved in 40 mL of acetone and 15 mL of distilled water and heated at reflux for 1h. The formation of complex was verified by the observation of AgCl precipitate. The resultant mixture was filtered and rotary evaporated. The brownish black precipitate was obtained by adding 2 mL of a 0.1 M NaClO₄ solution. Purification was achieved by column chromatography using Sephadex SP-C-25 as the column support and a 0.1 M NaClO₄ aqueous solution as the eluent. The second band was recovered from the column and this red solution was reduced in volume by rotary evaporator until a precipitate began to form. The solution was then cooled in refrigerator overnight and a red product was recovered by filtration. Yield: 90 mg (89%). Anal. Found (Calcd): C, 43.99 (44.33); H, 3.08 (3.17); N, 9.59 (9.57).

[(tpy)(phen)Ru(O)](ClO₄)₂. [(tpy)(phen)Ru(OH₂)](ClO₄)₂ (50 mg, 0.07 mmol) was dissolved in a 20 mL of distilled water. To the stirred solution was slowly added Ce (IV) (90 mg, 0.16 mmol) in 7 mL of a 1.0 M HClO₄. The yellow precipitate was filtered and washed well with iced water, then dried in a vacuum desiccator. Yield: 48 mg (96%). IR (KBr): $\nu_{\text{Ru=O}}=799\text{ cm}^{-1}$. Anal. Found (Calcd): 44.88 (45.58); H, 2.67 (2.69); N, 9.78 (9.84).

Instrumentation. Routine UV-visible spectra and slow kinetic runs were recorded on a Hewlett-Packard 8452A Diode Array spectrophotometer using HP 89532A general scanning and HP 89532K kinetics softwares. FT-IR spectra were obtained on a Bomem MB 100 FT-IR spectrophotometer as either on nujol mulls or in solutions using NaCl plates. Fast kinetic measurements were carried out by using a Photal RA-401 stopped-flow spectrophotometer. The system was interfaced with an IBM compatible computer system employing RA-451 data processor. The temperature of the solution was controlled within $\pm 0.2\text{ }^{\circ}\text{C}$ by using a Brinckman Lauda K-2/RD water bath circulator. All of the ¹H and ³¹P NMR data were obtained in a Varian Model Gemini-200 FT-NMR spectrometer using D₂O or CD₃CN as solvent. The chemical shift parameters were presented in parts per million (δ) downfield from internal reference tetramethylsilane (TMS) while the ³¹P chemical shifts were referenced to external 85% H₃PO₄. Cyclic voltametric experiments were conducted in a one-compartment cell equipped with Pt-gauze working electrode, a platinum-wire electrode, and the Ag/AgCl electrode at $25 \pm 2\text{ }^{\circ}\text{C}$ and were uncorrected for the junction potential effects.¹⁰ Cyclic voltammograms were obtained with a home-made potentiostat/galvanostat. In the coulometric determinations a Pt-gauze working electrode was used. Elemental analyses were performed by analytical laboratory at Basic Science Institute of Korea.

UV-Visible Measurements. The formation of [(tpy)(phen)Ru^{II}-NCCH₃]²⁺ and [(bpy)₂(*p*-tert-butylpy)Ru^{II}-NCCH₃]²⁺ was easily identified by dissolving corresponding each aqua complex in CH₃CN. Spectral changes with time showed that the half-life (*t*_{1/2}) of solvation reaction occurred in 15 min for [(tpy)(phen)Ru^{II}-OH₂]²⁺ and 50 min for [(bpy)₂(*p*-tert-butylpy)Ru^{II}-OH₂]²⁺.¹¹ Stoichiometric relationships in the

reaction between [(tpy)(phen)Ru^{IV}=O]²⁺ and [PPh₃] in CH₃CN were in part determined in a spectrophometric titration where the Ru(IV)/PPh₃ mole ratio was varied between 0 and 2 by adding different volumes of stock solution of PPh₃ to equal volumes of a Ru(IV) stock solution. No precautions were taken to exclude air. With the addition of PPh₃ solution, the visible absorption peak at 485 nm decreased in intensity with the increase of the peak at 456 nm of [(tpy)(phen)Ru^{II}-NCCH₃]²⁺. A mole ratio (PPh₃/Ru) against absorbance at 456 nm showed a linear ratio of 1.0. Continued addition of PPh₃ did not cause any increase in absorbance until an apparent end point at Ru/PPh₃=1.0 is observed. A blank solution of Ru(IV) without adding PPh₃ in CH₃CN showed no spectral changes in the visible region over a time span of several hours. Same experiments were performed for [(bpy)₂(*p*-tert-butylpy)Ru^{IV}=O]²⁺ oxidant toward PPh₃.

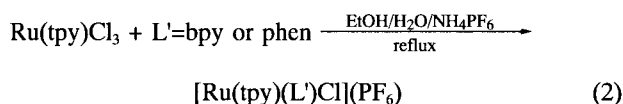
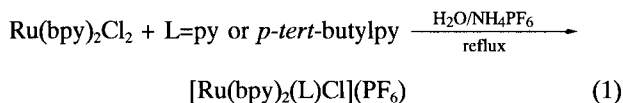
Infrared Measurements. To observe the infrared spectral changes that occur in the course of the reaction between PPh₃ and [(tpy)(phen)Ru^{IV}=O]²⁺ complex in CH₃CN, 5 mg of freshly recrystallized PPh₃ in 10 mL of CH₃CN (to give 1.9 mM solution) was added to 14 mg of solid [(tpy)(phen)Ru^{IV}=O]²⁺ (2.0 mM solution). The infrared spectra of solution in an approximately 1 mm pathlength NaCl was obtained at every min in the region 1300-1050 cm⁻¹. From the completely reacted (1 day old) solution, we confirmed P=O stretching frequency at 1195 cm⁻¹. Quantitative infrared analysis for OPPPh₃ was carried out by following the previous mentioned procedures.¹²

Kinetic Measurements. The oxidation of PPh₃ by [(tpy)(phen)Ru^{IV}(O)]²⁺ initially afforded an intermediate observed at the wavelength of 488 nm. The rate of the rapid reduction of Ru(IV) to Ru(II) intermediate was monitored from the absorbance change against time at 468 nm, which was an isosbestic point of the intermediate and the final solvolysis product, [(tpy)(phen)Ru^{II}-NCCH₃]²⁺ at 456 nm. Likewise, the oxidation of PPh₃ by [(bpy)₂(*p*-tert-butylpy)Ru^{IV}(O)]²⁺ initially afforded an intermediate observed at the wavelength of 478 nm. The rate of the rapid reduction of Ru(IV) to Ru(II) intermediate was monitored from the absorbance change against time at 456 nm, which was an isosbestic point of the intermediate and the final solvolysis product, [(bpy)₂(*p*-tert-butylpy)Ru^{II}-NCCH₃]²⁺ at 441 nm. Stopped-flow measurements of the rate of formation of the intermediate in the oxidation of PPh₃ and Ru(IV) were carried out on the Photal RA-401 stopped-flow apparatus as was described in Experimental Section. Pseudo-first-order condition was maintained throughout the experiments with PPh₃ in excess. Reported values of the rate constants were average of five or more experiments in which the same solutions reacted under the reaction conditions employed.

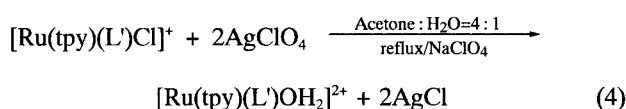
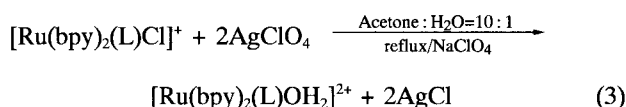
Results and Discussion

Syntheses. The preparations of the six-coordinate ruthenium and osmium complexes were reported by Dwyer and co-workers.¹³ The syntheses reported here represented alternative procedures for obtaining similar complexes. The mono-substituted complexes [Ru(bpy)₂(L)Cl]⁺ (L=py or *p*-tert-butylpy) and [Ru(tpy)(L)Cl]⁺ (L=bpy or phen) were

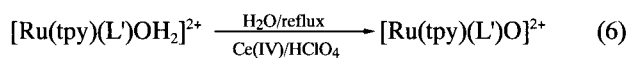
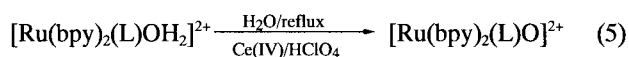
prepared by reaction of the free ligand either with *cis*-Ru(bpy)₂Cl₂ or with Ru(tpy)Cl₃ (eq. 1-2).



The ruthenium mono-aquo complex was easily achieved by exchange reaction using AgClO₄. Purification of the crude aquo complexes was accomplished by filtering off AgCl followed by precipitation using a saturated NaClO₄ solution (eq. 3-4). The aquation reaction was easily checked spectrophotometrically by monitoring the disappearance of the peak for [Ru(bpy)₂(L)Cl]⁺ or [Ru(tpy)(L')Cl]⁺ around λ_{max}=504-512 nm and the appearance of [Ru(bpy)₂(L)OH₂]²⁺ or [Ru(tpy)(L')OH₂]²⁺ peak at λ_{max}=474-476 nm. In several preparations, pure complexes were obtained through column chromatography.



The oxidation of [Ru^{II}-OH₂]²⁺ species with Ce(IV) to the corresponding Ru^{IV}=O species was performed in aqueous solution, in which the product spontaneously precipitated from a saturated NaClO₄ solution (eq. 5-6). Upon addition of Ce(IV) to an aqueous solution of [Ru^{II}-OH₂]²⁺, the red-colored mixture turned to a yellow color. The oxidation reaction was easily confirmed by monitoring the complete disappearance of MLCT band at λ_{max}=474-476 nm.



Stoichiometry. Using a mole ratio plot of the spectrophotometric titration data taken near the end of the reaction, a 1:1 mole relationship between [Ru^{IV}=O]²⁺ and added [PPh₃] in CH₃CN was established. Using the calibration curve for OPPh₃ as described in Experimental Section, free OPPh₃ formed from the completely reacted solutions of [Ru^{IV}=O]²⁺ and PPh₃ was determined as quantitative.

The UV-visible spectral changes during the reaction of [Ru^{IV}(tpy)(phen)(O)]²⁺ with PPh₃ in CH₃CN at room temperature are shown in Figure 1.

The initially featureless spectrum of [Ru^{IV}=O]²⁺ in visible region changed rapidly to give an intermediate with λ_{max}=485 nm upon addition of PPh₃. The subsequent spectral changes show the solvolysis of the intermediate by CH₃CN to yield [Ru^{II}-NCCH₃]²⁺ with λ_{max}=456 nm in eq. 7. The spectrum of the intermediate is typical of MLCT bands of other polypyridyl Ru(II) complexes.^{12,14,15} Similar spectral

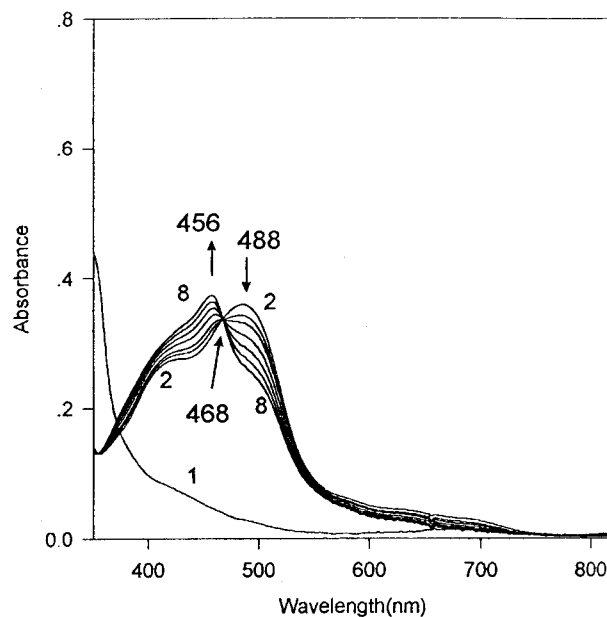
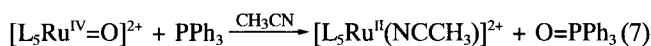


Figure 1. UV/VIS spectral changes observed during the oxidation of PPh₃ (7.6×10^{-4} M) by [Ru^{IV}(tpy)(phen)(O)](ClO₄)₂ (6.7×10^{-5} M) in CH₃CN: 1. [Ru^{IV}(tpy)(phen)(O)](ClO₄)₂ only; 2. 5 sec; 3. 30 min; 4. 1 hr; 5. 2 hr; 6. 3 hr; 7. 4 hr; 8. 6 hr.

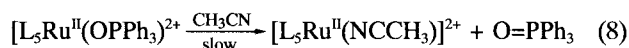
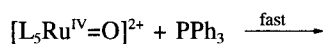
changes are obtained from the oxidation of PPh₃ by [(bpy)₂(*p*-*tert*-butylpy)Ru^{IV}(O)]²⁺ in CH₃CN at room temperature.

The overall reaction was



FT-IR Spectral Changes. Infrared spectral changes which parallel the changes in the UV-visible spectra are shown in Figure 2.

Shortly after [L₅Ru^{IV}=O]²⁺ and PPh₃ are mixed in acetonitrile, an intense peak observed at 1152-1158 cm⁻¹ is usually associated with the P=O stretching frequency of O-bound OPPh₃ to the metal.⁸ Over the long period of solvolysis reaction shown in Figure 2, the band of an intermediate peak decreases while the peak of free O=PPh₃ at 1195 cm⁻¹ increases. From the electronic and IR spectral characteristics of the intermediate, it seems clear that its structure is the OPPh₃ ligand bound to Ru(II), [L₅Ru^{II}-OPPh₃]²⁺. Because of the labile nature of the intermediate, it solvolyzes far slowly to give [L₅Ru^{II}-NCCH₃]²⁺ and O=PPh₃ (eq. 8).



Although the isolation of the intermediate from the alternate routes¹⁵ was not successful, the solids obtained did show the same electronic and IR spectral patterns. As is shown in Table 1, the P=O stretching band in [Ru^{II}-O=PPh₃]²⁺ intermediate from the reaction of [Ru^{IV}(bpy)₂(*p*-*tert*-butylpy)(O)]²⁺ and PPh₃ shifts to the lowest wavenumber. The presence of the bulky *tert*-butyl group in the ligand might be related to the great degree of the shift.

Labeling Studies. To find out possible sources of the oxygen that appears in the OPPh₃ product, a tracer study

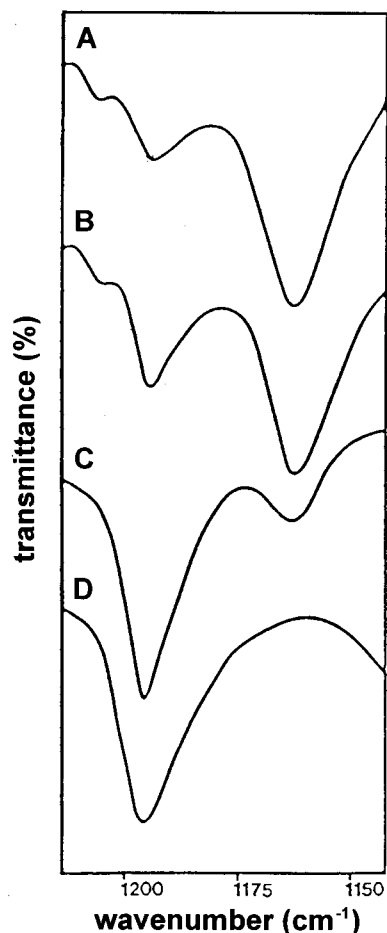


Figure 2. FT-IR spectra in CH_3CN solution that result from the oxidation of PPh_3 (0.026 mM) by $[\text{Ru}^{\text{IV}}(\text{tpy})(\text{phen})(\text{O})](\text{ClO}_4)_2$ (0.013 mM): A. 5 sec; B. 1.5 hr; C. 5 hr; D. 24 hr.

using ^{18}O -labeled oxidant was conducted. An experiment in which $[\text{Ru}^{\text{IV}}(\text{O})]^{2+}$ containing approximately 60 atom % $[\text{Ru}^{\text{IV}}(^{18}\text{O})]^{2+}$ was allowed to react with PPh_3 in CH_3CN and analyzed in the manner previously described.⁴ A quantitative analysis for $^{18}\text{OPPh}_3$ (1158 cm^{-1}) and $^{16}\text{OPPh}_3$ (1192 cm^{-1}) using data from two separate experiments showed essentially complete oxygen atom transfer from $[\text{Ru}(\text{O})]^{2+}$ to PPh_3 (60% ^{18}O product expected vs. 58% observed).

NMR Spectral Changes. The course of reaction that appears to occur is also corroborated with proton and phosphorous NMR spectrophotometers. In complexes of the

type of six coordinated $[(\text{bpy})_2(\text{py})\text{Ru}^{\text{II}}\text{-X}]^{2+}$ complexes, the chemical shift of the one of 6'-protons of the bipyridine that is the nearest to X is shifted furthest downfield. The peak is affected by the nature of X and also indicates the presence

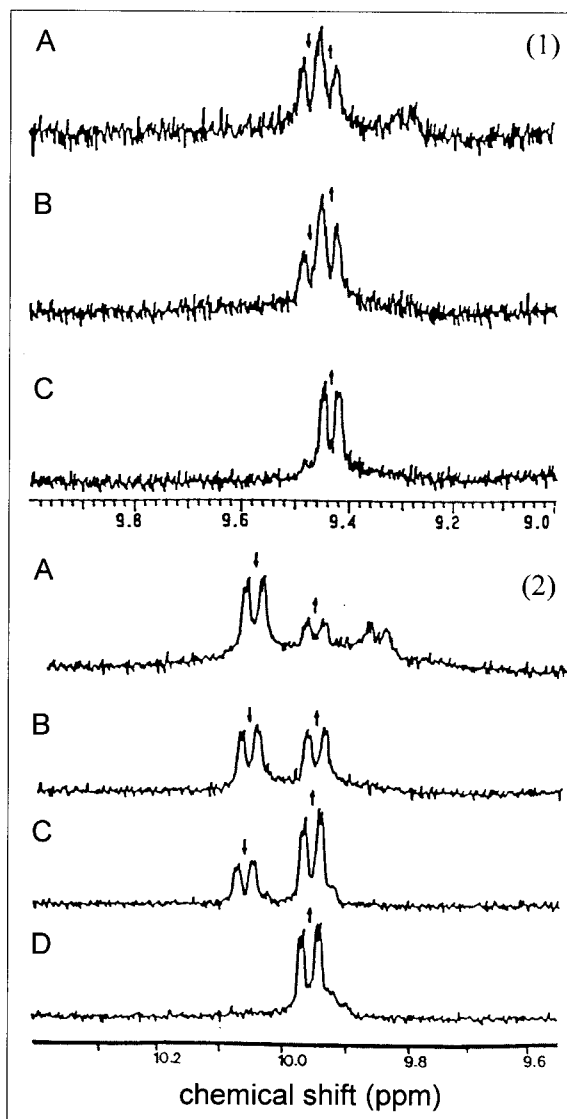


Figure 3. ^1H NMR spectral changes of a reaction mixture in CD_3CN containing (1) PPh_3 (0.042 M) and $[(\text{bpy})_2(p\text{-tert-butylpy})\text{Ru}(\text{O})]^{2+}$ (0.039 M): A. 10 min; B. 30 min; C. 4 hr. (2) PPh_3 (0.026 mM) by $[(\text{tpy})(\text{phen})\text{Ru}(\text{O})]^{2+}$ (0.013 mM): A. 10 min; B. 4 hr; C. 19 hr; D. 60 hr.

Table 1. The spectral data for the intermediates in the oxidation of PPh_3 in CH_3CN at $25\text{ }^\circ\text{C}$

Entry	Intermediate	Spectral data				Ref.
		UV/Vis λ_{max} , nm	FT-IR $\nu_{\text{P=O}}$, cm^{-1}	^1H NMR ^a δ , ppm	^{31}P NMR δ , ppm	
1	$[(\text{bpy})_2(\text{py})\text{Ru}^{\text{II}}\text{-OPPh}_3]^{2+}$	479	1150	9.45	50.1	12
2	$[(\text{bpy})_2(p\text{-tert-butylpy})\text{Ru-OPPh}_3]^{2+}$	478	1152	9.47	50.3	this work
3	$[(\text{tpy})(\text{bpy})\text{Ru}^{\text{II}}\text{-OPPh}_3]^{2+}$	485	1161	9.75	49.5	4
4	$[(\text{tpy})(\text{phen})\text{Ru}^{\text{II}}\text{-OPPh}_3]^{2+}$	488	1158	10.06	50.3	this work

^a the chemical shift observed in the region between 9.0 and 11.0 ppm.

of different ligand bound to Ru(II).^{15,16} Likewise, the chemical shift of the one of 6 or 6' proton of the bpy ligand in the complex of type $[(\text{tpy})(\text{bpy})\text{Ru}^{\text{II}}\text{-L}]^{2+}$ is also affected by the nature of the L.^{4,17} ¹H NMR spectral changes from the mixing of $[\text{Ru}(\text{tpy})(\text{phen})\text{O}]^{2+}$ and PPh_3 in CD_3CN shown in Figure 3 indicate the occurrence of resonances at 10.06 ppm and 9.96 ppm in addition to the peak at 9.88 ppm. Over the longer duration, the 10.06 ppm peak decreases with concomitant increase in the resonance at 9.96 ppm, which ascribes to the formation of $[\text{Ru}(\text{tpy})(\text{phen})(\text{NCCD}_3)]^{2+}$ complex. Finally the sole peak at 9.96 ppm was observed after 24 h. Similiar spectral behaviors have been observed for the oxidation PPh_3 by $[\text{Ru}^{\text{IV}}(\text{bpy})_2(p\text{-tert-butylpy})(\text{O})]^{2+}$ in CD_3CN , which shows the resonances at 9.47 ppm and 9.43 ppm in addition to the peak at 9.30 ppm. After 4 h, the 9.47 ppm peak decreases with concomitant increase in the resonance at 9.43 ppm which is attributed to the formation of $[\text{Ru}(\text{bpy})_2(p\text{-tert-butylpy})(\text{NCCD}_3)]^{2+}$ complex.

³¹P NMR spectroscopy was also used to deduce the nature of the intermediate. Figure 4 shows the appearance of the peak at 50.3 ppm, which is related to the intermediate from the reaction mixture of $[\text{Ru}^{\text{IV}}(\text{bpy})_2(p\text{-tert-butylpy})(\text{O})]^{2+}$ and PPh_3 . After the reaction was complete, only the resonance at 27.4 ppm for $\text{O}=\text{PPh}_3$ was observed. Similiar spectral changes have been obtained from the reaction between PPh_3 and $[\text{Ru}^{\text{IV}}(\text{tpy})(\text{phen})(\text{O})]^{2+}$ in CD_3CN . The peak which is related to the intermediate appeared at 50.3 ppm.

Table 1 summarizes the proton and phosphorous NMR results of the chemical shifts of the intermediates in the oxidation PPh_3 by $[\text{Ru}^{\text{IV}}(\text{O})]^{2+}$. Although there is no significant change in the chemical shift, there is a lower field shift by changing from the tpy-phen or tpy-bpy system to bis/bpy-py one from the ¹H NMR spectra. From the data in hand, bulky *tert*-butyl substituent at *para* position on bpy ligand did not affect the change in the chemical shift of the intermediate. Rather the chemical shift may be dictated largely by electronic effects from the comparison between entries 3 and 4.

Redox Properties. A cyclic voltammogram of $[\text{Ru}(\text{tpy})(\text{phen})\text{OH}_2]^{2+}$ in an aqueous solution buffered at pH 6.8 shows two distinct reversible redox waves. Similiar behaviors were observed for $[\text{Ru}(\text{tpy})(\text{bpy})\text{OH}_2]^{2+}$ and $[\text{Ru}(\text{bpy})_2(\text{L})\text{OH}_2]^{2+}$ (here L=py or *p-tert-butylpy*). Within the 10 > pH > 1.5 region, the potentials for the Ru(II/III) couple and the Ru(III/IV) couple form two straight lines, with slopes very close to the Nernstian prediction of -0.059 V/pH unit, indicative of a one-electron oxidation accompanied by the dissociation of one proton.^{7,10} The potentials for the other Ru(II/III) and Ru(III/IV) in Table 2

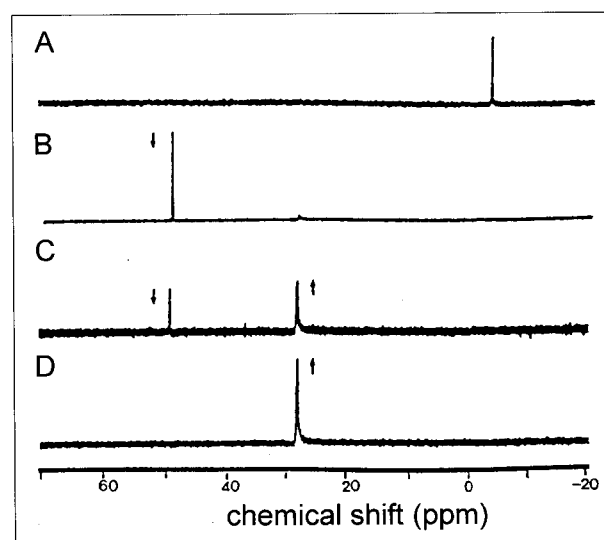


Figure 4. ³¹P NMR spectral changes of a reaction mixture in CD_3CN , which contained initially PPh_3 (0.026 M) and $[(\text{tpy})(\text{phen})\text{Ru}(\text{O})]^{2+}$ (0.013 M): A. PPh_3 ; B. 10 min; C. 19 hr; D. 60 hr.

are quite similiar. However, substitution of *p-tert-butyl-py* for py in bis/bpy-py system results in an increase in the oxidation potentials of approximately 0.06 V. Considering the ability of *p-tert-butyl-py* ligand to provide stronger coordination to the ruthenium metal, it is hardly explainable with a change in activation energy of oxygen atom transfer equal to ~ 4 kcal/mol.

Kinetics. The kinetics of formation of the intermediate in the oxidation of PPh_3 by $[\text{Ru}^{\text{IV}}(\text{O})]^{2+}$ in CH_3CN were monitored at the isobestic point of the disappearance of the intermediate and the appearance of $[\text{Ru}-\text{NCCH}_3]^{2+}$ for each oxidant using UV-vis spectroscopy. Rate constant data for the oxidation of PPh_3 by $[\text{Ru}^{\text{IV}}(\text{O})]^{2+}$ in CH_3CN at each temp are summarized in Table 2. Kinetic data were fit to a second-order model for $[\text{PPh}_3]$ and $[\text{Ru}^{\text{IV}}(\text{O})]^{2+}$. Previous kinetic studies support this assumption. The rate enhancement for bis/bpy-py system must be attributed to the presence of less sterically hindered pyridine ligand compared to bis/bpy-*p-tert-butylpy* one, which will also account for the rate difference between tpy-bpy and tpy-phen system.

Activation parameters for the reaction between $[\text{Ru}^{\text{IV}}(\text{O})]^{2+}$ and PPh_3 in CH_3CN were obtained from the plot of $\ln(k/T)$ vs $1/T$ over the temperature range of 15–40 °C. The results shown in Table 2 would not suggest the apparent change in mechanism for different oxidant. The higher activation energy for sterically hindered bis/bpy-*p-tert-butylpy* system against bis/bpy-py one was observed, although the difference is not significant.

Table 2. Summary of half-potential, kinetic and thermodynamic parameters for the oxidation of PPh_3 by four representative oxidants

Oxidant	Half-potential ^a	k_b	ΔH^\ddagger	ΔS^\ddagger	Ref.
$[(\text{bpy})_2(\text{py})\text{Ru}^{\text{IV}}=\text{O}]^{2+}$	0.42, 0.53	$1.75(\pm 0.10) \times 10^5$	$4.7(\pm 0.5)$	$-19(\pm 3)$	12
$[(\text{bpy})_2(p\text{-tert-butylpy})\text{Ru}^{\text{IV}}=\text{O}]^{2+}$	0.48, 0.61	$9.00(\pm 0.05) \times 10^{-1}$	$9.0(\pm 0.6)$	$-28(\pm 4)$	this work
$[(\text{tpy})(\text{bpy})\text{Ru}^{\text{IV}}=\text{O}]^{2+}$	0.49, 0.62	$1.25(\pm 0.08) \times 10^6$	$3.5(\pm 0.5)$	$-23(\pm 3)$	4
$[(\text{tpy})(\text{phen})\text{Ru}^{\text{IV}}=\text{O}]^{2+}$	0.48, 0.58	$1.49(\pm 0.16) \times 10^3$	$5.9(\pm 0.8)$	$-20(\pm 1)$	this work

^a potential values are vs SCE, T=25 °C, I=0.1 M, pH=7. ^b average of five determinations at a single concentration (T=25 °C).

The solvolysis rates were independent of the concentration of added PPh₃. The solvolysis rate for [Ru(tpy)(phen)OPPh₃]²⁺, k (25 °C)= 7.8×10^{-6} sec⁻¹ is slower than for [Ru(tpy)(bpy)OPPh₃]²⁺, k (25 °C)= 6.7×10^{-5} sec⁻¹. However the rate for [Ru(bpy)₂(*p*-*tert*-butylpy)OPPh₃]²⁺, k (25 °C)= 2.3×10^{-4} sec⁻¹ is quite similar to that for [Ru(bpy)₂(py)OPPh₃]²⁺, k (25 °C)= 1.5×10^{-4} sec⁻¹ within experimental error, which suggests the steric relief does not affect the solvolysis rate.

Mechanism. It is clear that the oxidation of PPh₃ by [Ru^{IV}=O]²⁺ in acetonitrile occurs by a net oxygen atom transfer. The final free products, [Ru^{II}-NCCH₃]²⁺ and O=PPh₃, are formed in quantitative yield by the sequence reactions shown in eq. 8. In an initial rapid step, the bound phosphine oxide complex, [Ru^{II}-OPPh₃]²⁺, is formed as a detectable intermediate followed by a far slower solvolysis reaction to afford the products. The results of the detection of the intermediate and the ¹⁸O-labelling experiment suggest that the transferred oxygen in O=PPh₃ is the oxyl group of the Ru(IV) oxidant.

There is a clear evidence for [Ru^{IV}=O]²⁺ acting as a 2e oxidant with oxo atom transfer to the reductant. The O-atom transfer reactivity suggests an electrophilic character at the oxo group. The electrophilic character is a shared property of the metal-oxo combination. In an electronic sense, the acceptor orbitals are largely d π (Ru) in character. The metal-based acceptor orbitals are strongly mixed with oxygen *p* orbitals, which promote the Ru-oxo interaction.¹⁹

We have previously discussed several mechanistic possibilities for the initial redox step.⁴ The oxidation reactivity toward PPh₃ by four representative Ru^{IV}=O²⁺ oxidants reported here will provide a more quantitative view of ruthenium mono-oxo oxidants toward PPh₃. Regarding the rate constant, the strongest oxidant is tpy-bpy system and the weakest one is bis/bpy-*p*-*tert*-butylpy and the ratio of the rate difference is surprisingly more than 10⁷!

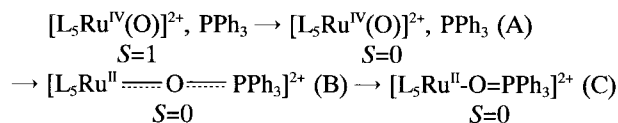
A negative value for ΔS^\ddagger suggests associative mechanism. The difference of 5 e.u. in ΔS^\ddagger does not simply explain the rate change. However, there is a big difference in activation enthalpy for [Ru(tpy)(bpy)(O)]²⁺ system (3.4 kcal/mol) against for [Ru(bpy)₂(*p*-*tert*-butylpy)(O)]²⁺ one (9.0 kcal/mol).

A magnetic study on the d⁴ [Ru^{IV}=O]²⁺ at room temperature shows that Ru(IV) oxidant has a "triplet" ground state with two unpaired electrons. Without considering the effects of spin-orbit coupling, the observation of two unpaired electrons is consistent with (d_{xy})²(d_{xz})(d_{yz})¹ where the Ru=O bond is taken as the *z* axis and the symmetry of the complex is assumed to be C_{4v}. Since the actual symmetry of the oxidant is C₁ rather than C_{4v}, the d_{xz} and d_{yz} orbitals are inequivalent and their degeneracy should be lifted. With the lifting of the degeneracy, it is not unreasonable to expect that a relatively low-lying "singlet" state having the electronic population (d_{xy})²(d_{yz})² might exist for [Ru^{IV}(O)]²⁺.

Since the initial intermediate in the redox step is the d⁶ Ru(II) complex with S=0, which has diamagnetic character, a spin state will decide the occurrence of the reaction quantum mechanically. It will also determine the rate in the redox step. The intermediate eventually produces diamagnetic [Ru^{II}(NCCH₃)]²⁺ complex with S=0.

A possible mechanism might be involved in the initial population of the S=0 reactant state followed by the thermal-

ly activated redox step. A spin change should be occurred in the preequilibrium step.



Such a preequilibrium step assumed to be very rapid, under our reaction conditions, no deviation from second-order kinetics was observed.

In the case of [Ru(bpy)₂(*p*-*tert*-butylpy)(O)]²⁺ complex, the presence of the bulky *tert*-butyl substituent requires more orientation and vibration to the thermally accessible reactant orientation in the associated complex. Because of a slow change in electronic distribution, there exists a precursor (B) before leading to the formation of an intermediate. This mechanism will be also applied to the sterically more strained tpy-phen system compared to tpy-bpy one.

The formation of the possible diamagnetic complex (B) in the slow step should be evidenced from the proton NMR spectral changes in Figure 3 which show additional peak at 9.30 ppm for [Ru(bpy)₂(*p*-*tert*-butylpy)(O)]²⁺ and at 9.88 ppm for [Ru(tpy)(phen)(O)]²⁺ in the oxidation of PPh₃.

Implications for Catalysis. Previous work has shown that the [Ru^{IV}=O]²⁺/[Ru^{II}-OH₂]²⁺ couples can be utilized as chemical and electrochemical oxidation catalysts toward a variety of organic and inorganic substrates.¹⁸ We have attempted to develop an electrocatalytic procedure for the oxidation of triphenylphosphine to triphenylphosphine oxide using four representative [(bpy)₂(*p*-*tert*-butylpy)Ru^{IV}=O]²⁺ oxidants. For example, electrocatalysis of an aqueous solution which was 0.08 M in PPh₃, 4 mM in [Ru^{IV}=O]²⁺, and 0.1 M in HPO₄²⁻/H₂PO₄⁻ buffer solution containing 50% by volume *tert*-butylalcohol as a solubilizing agent was carried out at 1.0 V (vs Ag/AgCl). Steady-state catalytic currents of 10 μ A were obtained by using three-compartment cell. The electrolysis was continued until 108 coulombs had passed as shown by integrating the area under the current-time curve. The amount of O=PPh₃ formed (100%) was verified from FT-IR spectroscopy.

Acknowledgment. This research was supported by the Korea Science and Engineering Foundation under Grant No. 96-0501-01-01-3.

References

- (a) Holm, R. H. *Chem. Rev.* **1987**, *87*, 1401. (b) Holm, R. H. *Coord. Chem. Rev.* **1990**, *100*, 183. (c) Laughlin, L. J.; Young, C. G. *Inorg. Chem.* **1996**, *35*, 1050.
- (a) Arasasingham, R. D.; He, G. X.; Bruice, T. C. *Ibid.* **1993**, *115*, 7985. (b) Khenkin, A. M.; Hill, C. L. *J. Am. Chem. Soc.* **1993**, *115*, 8178.
- Lee, K. A.; Nam, W. *J. Am. Chem. Soc.* **1997**, *119*, 1916 and references therein.
- Seok, W. K.; Kim, M. Y.; Yokomori, Y.; Hodgson, D. J.; Meyer, T. J. *Bull. Korean Chem. Soc.* **1995**, *16*, 619 and references therein.
- (a) Cheng, W.-C.; Yu, W.-Y.; Cheung, K.-K.; Che, C.-M. *J. Chem. Soc., Dalton Trans.* **1994**, *57*. (b) Welch, T. W.; Ciftan, S. A.; Whiye, P. S.; Thorp, H. H. *Inorg. Chem.* **1997**, *36*, 4812.

6. Dvletoglou, A.; Meyer, T. J. *J. Am. Chem. Soc.* **1994**, *116*, 215 and references therein.
7. Binstead, R. A.; Mcguire, M. E.; Dvletoglou, A.; Seok, W. K.; Roecker, L. E.; Meyer, T. J. *J. Am. Chem. Soc.* **1994**, *114*, 173.
8. Halmann, M.; Pinchas, S. *J. Chem. Soc.* **1958**, 3264.
9. Perrin, L. G.; Armarego, W. L. F.; Perrin, D. R. *Purification of Laboratory Chemicals*; Pergamon Press: New York, 1980.
10. Andrieux, C. P.; Blocman, C.; Dumas-Bouchiat, J. M.; M'Halla, F.; Saveant, J. M. *J. Electroanal. Chem. Rev.* **1980**, *113*, 19.
11. (a) Son, Y. J. M.S. Thesis, Dongguk Univ. 1994. (b) Moon, S. W. M.S. Thesis, Dongguk Univ. 1995.
12. Moyer, B. A.; Sipe, B. K. Meyer, T. J. *Inorg. Chem.* **1981**, *20*, 1475.
13. (a) Dwyer, F. P.; Good, H. A.; Cyrafas, E. C. *Aust. J. Chem. Rev.* **1963**, *16*, 544. (b) Bosnich, B.; Dwyer, F. P. *Aust. J. Chem.* **1966**, *19*, 2229.
14. Seok, W. K. *Bull. Korean Chem. Soc.* **1993**, *14*, 433.
15. Seok, W. K. Ph.D. Thesis, Univ. of North Carolina at Chapel Hill, 1988.
16. Roecker, E. L.; Dobson, J. C.; Vining, W. J.; Meyer, T. J. *Inorg. Chem.* **1987**, *26*, 779.
17. Gerli, A.; Reedijk, J.; Lakin, M. T.; Spek, A. L. *Inorg. Chem.* **1995**, *34*, 1836.
18. Thompson, M. S.; De Giovanni, W. F.; Moyer, B. A.; Meyer, T. J. *J. Org. Chem.* **1984**, *49*, 4972.
19. Powers, M. J.; Meyer, T. J. *J. Am. Chem. Soc.* **1980**, *102*, 1289.

Acid-Catalyzed Benzidine Rearrangement of Unsymmetrical Hydrazoaromatics

Koon Ha Park*, Moon-Kyeu Park, and Yoon Hwan Cho†

*Department of Chemistry, Chungnam National University, Taejon 305-765, Korea

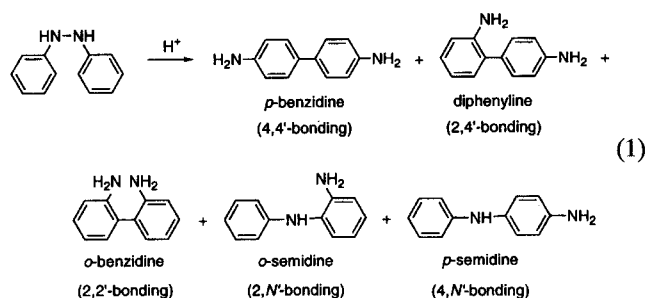
†Hanhyo Institute of Technology, Taejon 305-390, Korea

Received June 19, 1998

Acid-catalyzed benzidine rearrangements of new unsymmetrical diazanes **1-3**, prepared from the reduction of corresponding diazenes **4-6**, were carried out in ethanolic solutions. The results are as follows; rearrangement of (3-carbomethoxyphenyl)(3-methoxyphenyl)diazane **1** gave 4,4'-diamino-2-carbomethoxy-2'-methoxybiphenyl **12** (*p*-benzidine type) in 71% and 10-amino-3-methoxyphenanthridin-6(5*H*)-one **13**, 8-amino-3-methoxyphenanthridin-6(5*H*)-one **14** in 7.1% and 3.4%, respectively. Product **13** and **14** were formed by the condensation reaction of primarily formed *o*-benzidine and diphenylene type product, respectively. (5-Carbomethoxy-2-chlorophenyl)(4-methoxyphenyl)diazane **2** and (5-carbomethoxy-2-methylphenyl)(4-methoxyphenyl)diazane **3** underwent mainly disproportionations to give fission amines and corresponding diazenes in about 53% and 40% yields, respectively. The results obtained from the rearrangements of diazanes **1-3** indirectly indicated the importance of disproportionations to understand the benzidine rearrangements. The structures of benzidine rearrangement products were determined by usual NMR techniques such as DEPT, 2D H-H COSY, H-C COSY, 2D NOESY, and Gaussian function multiplication.

Introduction

Acid-catalyzed benzidine rearrangement has been studied extensively for more than 130 years since the rearrangement was discovered accidentally by Hofmann in the reduction of azobenzene.¹ Benzidine rearrangements refer to reactions in which diazanes are converted to two kinds of products in the presence of acid (eq. 1).²



One kind comprises diaminobiphenyl compounds such as benzidine (4,4'-bonding), diphenylene (2,4'-bonding), and *o*-benzidine (2,2'-bonding). In the other are aminodiphenylamine derivatives such as *o*-semidine (2,*N'*-bonding) and *p*-semidine (4,*N'*-bonding). Also formed are disproportionation products such as azobenzenes and arylamines, which are unavoidable in the usual benzidine rearrangements. At present it has been well established, by heavy atom kinetic isotope effects, that the rearrangement follow the patterns of the sigmatropic shifts.³ Recently, a [9,9]-sigmatropic shift in the acid-catalyzed benzidine rearrangement of bis[4-(2-furyl)phenyl]diazane was discovered, supporting that the benzidine rearrangement follow the patterns for sigmatropic processes.⁴ Described herein are benzidine rearrangements of new unsymmetrically substituted diazanes **1-3** containing carbomethoxy and methoxy groups separately at *meta* and *meta/para* positions of benzene rings. This work was undertaken in order to study the effects of unsymmetrical